

Statistics of Two-Phase Coupling in Turbulent Spherically Expanding Flames in Mono-sized Fuel-Droplet Mists

Gulcan Ozel Erol¹, Josef Hasslberger², Nilanjan Chakraborty¹

¹School of Engineering, Newcastle University, Newcastle-Upon-Tyne, Tyne and Wear, UK

²Bundeswehr University, Munich, Werner-Heisenberg-Weg 39, 85577 Neubiberg, Germany

1 Introduction

Turbulent combustion of droplet-laden mixtures involves complex interactions between combustion, heat transfer, droplet evaporation and fluid turbulence. A thorough knowledge of the interaction between liquid droplets and carrier gaseous phase is necessary for the purpose of fundamental understanding and modelling flame-droplet interaction. The experimental observations for spherically expanding spray flames revealed that flame-turbulence interaction is strongly affected by droplet diameter and the overall equivalence ratio [1]. Recent advancements in high-performance computing have enabled carrier phase Direct Numerical Simulations (DNS) to analyse different aspects of turbulent combustion processes in droplet-laden mixtures [2,3]. Previous DNS analyses [2,3] indicated that the gaseous phase combustion takes place predominantly in fuel-lean mode even for the overall (i.e. gaseous and liquid phases) fuel-rich fuel-air mixtures because of the differences in time-scales for evaporation and chemical reactions, which in turn affect the resulting combustion and mixing processes. A thorough understanding of the aforementioned behaviour and its influence on the subsequent combustion processes necessitate a detailed analysis of the interaction between liquid and gaseous phases, which serves as the motivation for the current analysis. To meet this objective, a DNS database of spherically expanding flames propagating into mono-sized fuel-droplet mists for a range of different initial droplet diameters and overall equivalence ratios has been considered here to analyse the statistics of liquid and gaseous phase interactions in turbulent combustion in droplet-laden mixtures.

2 Mathematical Background and Numerical Implementation

A modified single-step Arrhenius-type chemical mechanism, where the activation energy and the heat of combustion are taken to be functions of the gaseous equivalence ratio ϕ_g , is used for this analysis to keep computational demand for a detailed parametric analysis within reasonable limits. This chemical mechanism yields a realistic ϕ_g dependence of the unstrained laminar burning velocity $S_b(\phi_g)$ in hydrocarbon-air flames. The Lewis numbers of all species are assumed to be unity and all species in the gaseous phase are taken to be perfect gases. Standard values have been considered for the ratio of specific heats ($\gamma =$

$C_p^g/C_v^g = 1.4$, where C_p^g and C_v^g are the gaseous specific heats at constant pressure and volume, respectively) and Prandtl number ($Pr = \mu C_p^g/\lambda = 0.7$ where μ is the dynamic viscosity and λ is the thermal conductivity of the gaseous phase). The quantities transported for each droplet are computed in a Lagrangian approach, which are given as [2,3]:

$$\frac{d\vec{x}_d}{dt} = \vec{u}_d; \quad \frac{d\vec{u}_d}{dt} = \frac{\vec{u}(\vec{x}_d, t) - \vec{u}_d}{\tau_d^u}; \quad \frac{da_d^2}{dt} = -\frac{a_d^2}{\tau_d^p}; \quad \frac{dT_d}{dt} = \frac{T(\vec{x}_d, t) - T_d - B_d L_v / C_p^g}{\tau_d^T} \quad (1)$$

where L_v is the latent heat of vaporization, and τ_d^u , τ_d^p and τ_d^T are relaxation timescales for droplet velocity, diameter and temperature respectively, which can be expressed as: $\tau_d^u = \rho_d a_d^2 / (18 C_u \mu)$; $\tau_d^p = (\rho_d a_d^2 / 4\mu)(Sc/Sh_c)/\ln(1+B_d)$ and $\tau_d^T = (\rho_d a_d^2 / 6\mu)(Pr/Nu_c)[B_d/\ln(1+B_d)](C_p^l/C_p^g)$. Here, ρ_d is the droplet density, Sc is the Schmidt number, C_p^l is the specific heat for the liquid phase, $C_u = 1 + Re_d^{2/3}/6$ is the corrected drag coefficient, Re_d is the droplet Reynolds number, B_d is the Spalding number, Sh_c is the corrected Sherwood number and Nu_c is the corrected Nusselt number, which are given as [2,3]: $Re_d = \rho|\vec{u}(\vec{x}_d, t) - \vec{u}_d|a_d/\mu$; $B_d = [Y_F^s - Y_F(\vec{x}_d, t)]/(1 - Y_F^s)$ and $Sh_c = Nu_c = 2 + 0.555 Re_d Sc / (1.232 + Re_d Sc^{4/3})^{1/2}$ where Y_F^s is the value of fuel mass fraction Y_F at the surface of the droplet. The Clausius–Clapeyron equation for the partial pressure of the fuel vapour at the droplet surface p_F^s is used to evaluate the Spalding number B_d , which leads to the following expressions:

$$p_F^s = p_{ref} \exp(L_v/R [(1/T_{ref}^s) - (1/T_d^s)]); \quad Y_F^s = (1 + (W_A/W_F)[p(\vec{x}_d, t)/p_F^s - 1])^{-1} \quad (2)$$

where T_{ref}^s is the boiling point of the fuel at pressure p_{ref} and T_d^s is assumed to be T_d , and W_A and W_F are the molecular weights of air and fuel, respectively. The coupling between liquid and gaseous phases is provided by additional source terms in the gaseous transport equations as follows [2,4]:

$$\partial(\rho\varphi)/\partial t + \partial(\rho u_j \varphi)/\partial x_j = \partial[R_\varphi \partial\varphi_1/\partial x_j]/\partial x_j + \dot{\omega}_\varphi + \dot{S}_\varphi \quad (3)$$

where $\varphi = \{1, u_i, e, Y_F, Y_O\}$ and $\varphi_1 = \{1, u_i, T, Y_F, Y_O\}$ for the conservation equations of mass, momentum, energy, and mass fractions, respectively and $R_\varphi = \rho\nu/\sigma_\varphi$ for $\varphi = \{1, u_i, Y_F, Y_O\}$ and $R_\varphi = \lambda$ for $\varphi = e$, respectively, u_i is the velocity in the i^{th} direction, and T is the instantaneous dimensional temperature. The $\dot{\omega}_\varphi$ term corresponds to reaction rate and \dot{S}_φ is the appropriate source term due to droplet evaporation, which is tri-linearly interpolated from the droplet's sub-grid position, \vec{x}_d , to the eight surrounding nodes. Other variables are ν , kinematic viscosity, and σ_φ , an appropriate Schmidt number corresponding to φ . The droplet source term for any variable φ is expressed as [2,3]:

$$\dot{S}_\varphi = -(1/V) \sum_d d(m_d \varphi_d)/dt \quad (4)$$

where, V is the cell volume, $m_d = \rho_d(1/6)\pi a_d^3$ is the droplet mass.

A reaction progress variable c , based on oxygen mass fraction, Y_O and mixture fraction, $\xi = (Y_F - Y_O/s + Y_{O\infty}/s)/(Y_{F\infty} + Y_{O\infty}/s)$ can be written in the following manner [3]:

$$c = [(1 - \xi)Y_{O\infty} - Y_O]/[(1 - \xi)Y_{O\infty} - \max(0, \{\xi_{st} - \xi\}/\xi_{st})Y_{O\infty}] \quad (5)$$

where $Y_{O\infty} = 0.233$ is the oxygen mass fraction in air and $Y_{F\infty} = 1.0$ is the fuel mass fraction in the pure fuel stream. Considering n-heptane, C_7H_{16} as the fuel in the analysis, $s = 3.52$ denotes the stoichiometric mass ratio of oxidiser to fuel and $Y_{Fst} = \xi_{st} = 0.0621$ represents the corresponding fuel mass fraction and mixture fraction, respectively.

The transport equation of c can be obtained by using the transport equations for oxygen mass fraction, Y_O and mixture fraction, ξ in the following manner [3]:

$$\partial(\rho c)/\partial t + \nabla \cdot (\rho \vec{u} c) = \nabla \cdot (\rho D \nabla c) + \dot{w}_c + \dot{A}_c + S_c^* \quad (6)$$

where D is the molecular diffusivity and $\nabla \cdot (\rho D \nabla c)$ is the molecular diffusion term. Here, \dot{w}_c is the reaction rate, $\dot{S}_c^* = \dot{S}_c + \Gamma_m c$ is the source/sink term arising due to droplet evaporation and \dot{A}_c is the cross-scalar dissipation term arising due to mixture inhomogeneity which can be written as:

$$\dot{w}_c = -\xi_{st} \dot{w}_o / [Y_{O\infty} \xi (1 - \xi_{st})] \text{ for } \xi \leq \xi_{st}; \dot{w}_c = -\dot{w}_o / [Y_{O\infty} (1 - \xi)] \text{ for } \xi > \xi_{st} \quad (7)$$

$$\dot{S}_c = -\xi_{st} / (Y_{O\infty} \xi^2 (1 - \xi_{st})) [\xi \dot{S}_O + (Y_{O\infty} - Y_O) \dot{S}_\xi] \text{ for } \xi \leq \xi_{st}; \quad (8)$$

$$\dot{S}_c = -1 / (Y_{O\infty} (1 - \xi)^2) [(1 - \xi) \dot{S}_O + Y_O \dot{S}_\xi] \text{ for } \xi > \xi_{st}$$

$$\dot{A}_c = 2\rho D \nabla \xi \cdot \nabla c / \xi \text{ for } \xi \leq \xi_{st}; \dot{A}_c = -2\rho D \nabla \xi \cdot \nabla c / (1 - \xi) \text{ for } \xi > \xi_{st} \quad (9)$$

where \dot{w}_o is the reaction rate of oxidiser, $\dot{S}_\xi^* = \dot{S}_\xi + \Gamma_m \xi$ is the droplet source/sink term in the mixture fraction transport equation (i.e. $\partial(\rho \xi)/\partial t + \nabla \cdot (\rho \vec{u} \xi) = \nabla \cdot (\rho D \nabla \xi) + \dot{S}_\xi^*$) with $\dot{S}_\xi = (\dot{S}_F - \dot{S}_O/s)/(Y_{F\infty} + Y_{O\infty}/s)$, where $\dot{S}_F = \Gamma_m (1 - Y_F)$ and $\dot{S}_O = -\Gamma_m Y_O$ are the droplet source/sink terms in the species transport equation for fuel and oxidiser, respectively and Γ_m is the source term in the mass conservation equation due to evaporation. In the present analysis, the statistical behaviours of the source terms $\dot{S}_\rho = \Gamma_m$, \dot{S}_{u_i} , \dot{S}_e , \dot{S}_c^* and \dot{S}_ξ^* , which arise in the carrier phase transport equations due to droplet evaporation, will be analysed.

The DNS database used for this analysis is generated using a three-dimensional compressible code SENGAs [3,4], which adopts high order finite-difference and explicit third-order Runge-Kutta schemes for spatial discretisation and explicit temporal advancement, respectively. All these boundaries are assumed to be partially non-reflecting of the cubic domain of size $84.49\delta_z \times 84.49\delta_z \times 84.49\delta_z$ where $\delta_z = \alpha_{T_0}/S_b(\phi_g=1)$ is the Zel'dovich flame thickness with α_{T_0} being the thermal diffusivity in the unburned gas. The simulation domain is discretised by a uniform Cartesian grid of $(512)^3$, which ensures about 10 grid points within the unstrained thermal laminar flame thickness of the stoichiometric mixture $\delta_{st} = (T_{ad}(\phi_g=1) - T_0)/\max|\nabla T|_L$ where T_0 is the unburned gas temperature and $T_{ad}(\phi_g=1)$ is the adiabatic flame temperature of the stoichiometric mixture. The reacting flow field is initialised using the steady laminar solutions from COSILAB for different initial droplet diameters a_d and overall equivalence ratios ϕ_{ov} as detailed in a previous analysis [4]. A perfectly spherical kernel flame is placed at the centre of domain and an incompressible homogeneous isotropic velocity field is superimposed on the laminar spherical flames when the radius of the fully burned gas region (i.e. the region corresponding to reaction progress variable c value greater than 0.99) r_0 reaches $2\delta_{st}$ (i.e. $r_0/\delta_{st} = 2.0$). The unburned gas temperature T_0 is assumed to be 300 K and this implies a heat release parameter of $\tau = (T_{ad}(\phi_g=1) - T_0)/T_0 = 6.54$. The turbulent flame simulations are carried out for an initial value of normalised root-mean-square (rms) turbulent velocity $u'/S_b(\phi_g=1) = 4.0$ with a non-dimensional longitudinal integral length-scale of $L_{11}/\delta_{st} = 2.5$, and they have been continued for at least 2.1 chemical time scale (i.e. $2.1t_{chem} = 2.1\alpha_{T_0}/S_b^2(\phi_g=1)$), which corresponds to about 2.0 initial eddy turnover time (i.e. L_{11}/\sqrt{k} where k is the kinetic energy evaluated over the whole domain). The initial droplet number density ρ_N varies between $1.38 \leq (\rho_N)^{1/3} \delta_{th} \leq 2.07$ in the unburned gas, and the liquid volume fraction remains well below 0.01. The droplet diameter remains smaller than the Kolmogorov length scale η for all cases (i.e. $a_d/\eta = 0.15, 0.19, 0.23$ for the cases of $a_d/\delta_{st} = 0.04, 0.05, 0.06$ respectively). These values are comparable to those used in several previous analyses.

3 Results and Discussion

The statistically spherical flames in mono-sized droplet-mists are visualised by reaction progress variable isosurface $c=0.5$ for various ϕ_{ov} after $2.1t_{chem}$. As can be seen from Fig. 1, flames are wrinkled due to the effects of turbulence and the case with $\phi_{ov} = 0.8$ has a smaller volume of $c \geq 0.5$ than the corresponding $\phi_{ov} = 1.0$ and 1.2 cases. The probability density functions (PDFs) of the normalised magnitude of the velocity difference between the droplets and the surrounding carrier gas (known as slip velocity), $\Delta U_{slip} = |\vec{u}(\vec{x}_d, t) - \vec{u}_d|/S_b(\phi_g=1)$, are presented in Fig. 2a for different regions within the flame. These PDFs are computed using samples from the droplet positions for different ranges of c . It can be seen from Fig. 2a that the probability of obtaining higher magnitude of ΔU_{slip} increases with increasing droplet diameter. The maximum value of ΔU_{slip} remains close to unity for all values of ϕ_{ov} in the cases with the initial droplet diameter $a_d/\delta_{st} = 0.04$ except for the rear end of the reaction zone (i.e. $0.7 \leq c \leq 0.9$) in the $\phi_{ov} = 0.8$ case due to the combination of a small droplet number density and relatively rapid evaporation of small droplets. Furthermore, the PDFs of ΔU_{slip} peak at zero value for small droplets. For larger droplets (e.g. initial $a_d/\delta_{st} = 0.06$ cases) the PDFs of ΔU_{slip} show a wider distribution in the reaction zone of the flame but the distributions of ΔU_{slip} remain mostly insensitive to the variations of ϕ_{ov} .

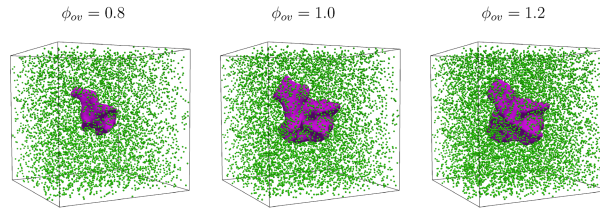


Figure 1. Instantaneous isosurfaces of reaction progress variable $c=0.5$ for $\phi_{ov} = 0.8, 1.0$ and 1.2 cases with initial $a_d/\delta_{st} = 0.06$ at $2.1t_{chem}$.

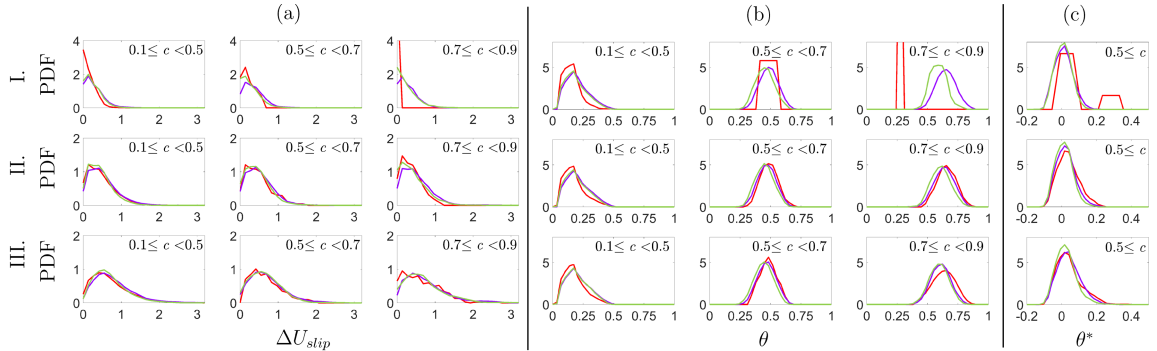


Figure 2. PDFs of (a) ΔU_{slip} (b) $\theta = (T - T_d)/(T_{ad}(\phi_g=1) - T_0)$ and (c) $\theta^* = \{T(\vec{x}_d, t) - T_d - B_d L_v / C_P^g\} / (T_{ad}(\phi_g=1) - T_0)$ on different c ranges for different $\phi_{ov} = 0.8$ (—), $\phi_{ov} = 1.0$ (—) and $\phi_{ov} = 1.2$ (—) cases and for different initial droplet radii $a_d/\delta_{st} = 0.04$ (I.), $a_d/\delta_{st} = 0.05$ (II.) and $a_d/\delta_{st} = 0.06$ (III.) with initial turbulence intensity $u'/S_b(\phi_g=1) = 4.0$.

Figure 2b shows the PDFs of non-dimensional temperature difference between droplets and surrounding gaseous phase, θ for different ranges of c . In the preheat zone (i.e. $0.1 \leq c \leq 0.5$), θ remains smaller than 0.5 for all cases considered here. As droplets move further towards the reaction zone, the most probable values of θ increase for the initial $a_d/\delta_{st} = 0.05$ and 0.06 cases for all values of ϕ_{ov} and also for the initial

$a_d/\delta_{st} = 0.04$ case for $\phi_{ov} = 1.0$ and 1.2, which suggests that the droplets in these cases may not fully evaporate even when the reaction zone is approached and this eventually gives rise to predominantly fuel-lean mixture in the gaseous phase. In the initial $a_d/\delta_{st} = 0.04$ case for $\phi_{ov} = 0.8$, the PDF of θ at the rear end of reaction zone is found to be narrower and the most probable value of θ has been found to be smaller than the corresponding $\phi_{ov} = 1.0$ and 1.2 cases. Due to smaller number density, the number of droplets which survive in the reaction zone, and the gaseous phase equivalence ratio ϕ_g remain small in the $\phi_{ov} = 0.8$ case with initial $a_d/\delta_{st} = 0.04$ in comparison to those in the corresponding $\phi_{ov} = 1.0$ and 1.2 cases. This leads to smaller burned gas temperature (not shown here) and consequently smaller most probable value and narrower PDF of θ in the $\phi_{ov} = 0.8$ case with initial $a_d/\delta_{st} = 0.04$ than in the corresponding $\phi_{ov} = 1.0$ and 1.2 cases.

Source terms associated with droplet evaporation in gaseous phase transport equations can be used to assess the flame-droplet interactions and to understand the contribution of droplets to the Eulerian phase transport equations of momentum, energy and scalars such as mixture fraction and reaction progress variable. Scatter plots of the normalised source term in the mass conservation equation $\Gamma_m \times \delta_{st}/\rho_0 S_b(\phi_g=1)$ coloured by normalised source terms in momentum transport equations $\{\dot{S}_{u_1}, \dot{S}_{u_2}, \dot{S}_{u_3}\} \times \delta_{st}/\rho_0 S_b^2(\phi_g=1)$ are presented in Fig. 3a-c. The mean values of $\Gamma_m \times \delta_{st}/\rho_0 S_b(\phi_g=1)$ conditional on c are shown by the black lines. As expected, small droplets with initial $a_d/\delta_{st} = 0.04$ mostly complete their evaporation within the flame front and this leads a weaker flame-droplet interaction in comparison to the large droplet cases. The $\phi_{ov} = 0.8$ cases exhibit negligible droplet contributions on the burned gas side due to small number density. Additionally, strong negative and positive contributions of $\{\dot{S}_{u_1}, \dot{S}_{u_2}, \dot{S}_{u_3}\} \times \delta_{st}/\rho_0 S_b^2(\phi_g=1)$ are found predominantly in unburned gas region where high values of $\Gamma_m \times \delta_{st}/\rho_0 S_b(\phi_g=1)$ exist.

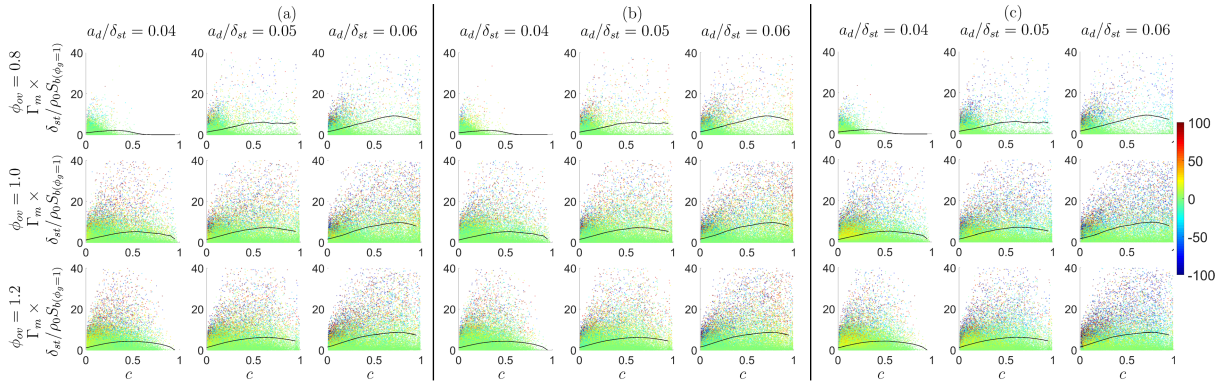


Figure 3. Scatter of $\Gamma_m \times \delta_{st}/\rho_0 S_b(\phi_g=1)$ as a function of c coloured with (a) $\dot{S}_{u_1} \times \delta_{st}/\rho_0 S_b^2(\phi_g=1)$, (b) $\dot{S}_{u_2} \times \delta_{st}/\rho_0 S_b^2(\phi_g=1)$ and (c) $\dot{S}_{u_3} \times \delta_{st}/\rho_0 S_b^2(\phi_g=1)$ for different values of ϕ_{ov} . Black line shows the variation of the mean values of $\Gamma_m \times \delta_{st}/\rho_0 S_b(\phi_g=1)$ conditional on c in Figs. 3 and 4.

The contributions of source terms (i.e. \dot{S}_e , \dot{S}_c^* and \dot{S}_ξ^*) associated with droplet evaporation to related gaseous transport equations of energy, reaction progress variable and mixture fraction are shown in Figs. 4a-c, respectively. Figure 4a shows that $\dot{S}_e \times \delta_{st}/\rho_0 C_p T_0 S_b(\phi_g=1)$ is generally negative in unburned gas side whereas the trend changes in burned gas to positive values because some of droplets which escape through the flame and reach the burned gas side due to turbulent fluid motion and get heated up. Some of these droplets are brought back into the flame from the burned gas by turbulent vortical motion, and eventually heat up the carrier gaseous phase due to $\theta^* < 0$, which can be substantiated from the PDFs of θ^* in Fig. 2c.

Figure 4b reveals that droplet evaporation has little influence on the transport equation of c but $\dot{S}_c^* \times \delta_{st}/\rho_0 S_b(\phi_g=1)$ becomes stronger for larger droplets in the preheat zone. Figure 4c reveals that the contribution of droplet evaporation to the mixture fraction transport equation \dot{S}_ξ^* increases with increasing Γ_m and this contribution strengthens with increasing droplet diameter.

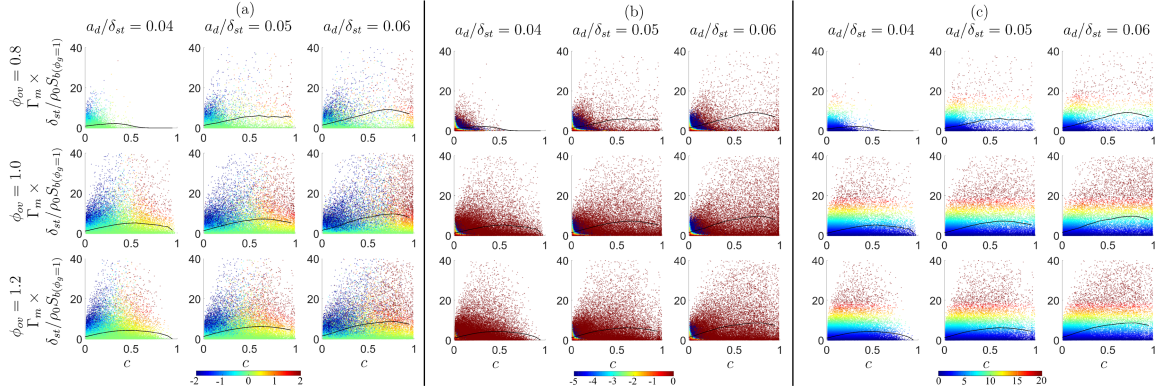


Figure 4. Scatter of $\Gamma_m \times \delta_{st}/\rho_0 S_b(\phi_g=1)$ as a function of c coloured with (a) $\dot{S}_e \times \delta_{st}/\rho_0 C_p T_0 S_b(\phi_g=1)$, (b) $\dot{S}_c^* \times \delta_{st}/\rho_0 S_b(\phi_g=1)$ and (c) $\dot{S}_\xi^* \times \delta_{st}/\rho_0 S_b(\phi_g=1)$ for different values of ϕ_{ov} .

4 Conclusions

A three-dimensional DNS database of spherically expanding flames propagating in mono-sized fuel-droplet mists for different overall equivalence ratios and droplet diameters has been utilised to analyse flame-droplet interaction in terms of the source terms associated with droplet evaporation in various gaseous carrier phase transport equations. It has been found that the slip velocity is significantly affected by the droplet size. Furthermore, evaporation contributions have significant influences on mass, momentum, energy and mixture fraction transport equations but this influence is relatively weak for the reaction progress variable transport equation.

Acknowledgements

The authors are grateful to EPSRC for financial and ARCHER and Rocket-HPC for computational support.

References

- [1] Lawes M, Saat A. (2011). Burning rates of turbulent iso-octane aerosol mixtures in spherical flame explosions. Proc. Combust. Inst. 33: 2047.
- [2] Reveillon J, Vervisch L. (2000). Spray vaporization in nonpremixed turbulent combustion modeling: a single droplet model. Combust. Flame 121: 75.
- [3] Wacks D. et al. (2016). Statistical Analysis of Turbulent Flame-Droplet Interaction: A Direct Numerical Simulation Study. Flow, Turbul. Combust. 96: 573.
- [4] Ozel Erol G. et al. (2018). A direct numerical simulation analysis of spherically expanding turbulent flames in fuel droplet-mists for an overall equivalence ratio of unity. Phys. Fluids. 30, 086104.